

High-Resolution Solution NMR Spectra in Inhomogeneous Magnetic Fields

Shuhui Cai*, Wen Zhang and Zhong Chen

Department of Physics, State Key Laboratory of Physical Chemistry of Solid Surface, Xiamen University, Xiamen 361005, China

Abstract: A high-resolution NMR spectrum, containing fine structures such as chemical shifts and scalar-coupling multiplet patterns, is helpful for analyzing molecular composition and structure. However, there are many cases where the magnetic environments are inhomogeneous, which may lead to severe signal overlapping and blur useful spectral information in liquid samples. Recently, many NMR techniques have been proposed to regain high-resolution spectral information in inhomogeneous magnetic fields. They can be mainly classified into three types that based on intermolecular multiple-quantum coherences, nutation echoes, and spatial encoding respectively. These methods can be applied to a wide range of samples, thereby opening a way to high-resolution *in vivo* and *ex situ* NMR spectroscopy. In this review, recent developments of these methods are presented and their applicability and efficiency are analyzed.

Keywords: High-resolution NMR spectroscopy, Inhomogeneous magnetic fields, Intermolecular multiple-quantum coherences, Nutation echo, Spatial encoding.

1. INTRODUCTION

Nuclear magnetic resonance (NMR) is an extremely versatile form of spectroscopy because of its precision, selectivity and non-invasiveness. From biomolecules to living organisms, from nanoparticles to materials, NMR spectroscopy has provided a wealth of invaluable information. This information generally comes from high-resolution NMR spectra containing fine structures of chemical shifts and scalar-coupling multiplet patterns.

For proton NMR of a liquid sample, homogeneity of the static magnetic field in the order of 10^{-8} is often required to obtain chemical shift and scalar coupling information [1]. However, there are many circumstances, where the magnetic fields vary spatially or temporally and cannot be well shimmed by a conventional field shimming method. For example, heterogeneous samples such as tissues, rock samples, and porous resin beads are subject to variation in magnetic susceptibility over the sample volume and between various components. Tissues with microscopic air inclusion such as lungs of mammals or leaves of plants, and interfaces between tissue and air or bone, are generally recognized to be inaccessible or very difficult for high-resolution NMR spectroscopy. In addition, there are intrinsically inhomogeneous designs such as inside-out or single-sided magnets. The inhomogeneous broadening due to magnetic susceptibility discontinuity and inhomogeneous magnetic field may be tens or hundreds of times greater than the homogeneous linewidth, leading to severe signal overlapping and loss of fine spectral features.

In order to regain the lost spectral information even in the presence of an inhomogeneous magnetic field, a variety of

techniques have been devised. These can be classified into two classes. One class is to improve the hardware [2]. For example, magnetic-angle spinning (MAS) was developed to remove line broadening caused by chemical-shift anisotropy and magnetic susceptibility discontinuity. Recently, Varian Nano-NMR probe was specifically designed to exploit MAS for a very small amount ($\leq 40\mu\text{L}$) of sample, which has provided a valuable tool to dramatically improve resolution and sensitivity of proton signals obtained from support-bounded compounds [3]. Blümich and co-workers designed a magnet array to generate a volume of highly homogeneous magnetic field external to the portable single-sided NMR magnet with a spectral resolution of 0.25 ppm for localized ^1H NMR spectra [4, 5]. At the same time, many methods such as linear programming (LP) algorithms [6] and stream functions [7] were used to design shimming coils. A combined approach of passive (ferromagnetic) and active (electronic) shimming was developed to generate strong and highly-accurate homogeneous fields for *in vivo* NMR spectroscopy at a high field system where the electronic shimming may be insufficient to permit homogenization at desired spatial scale [8].

Another class is to exploit new experimental techniques or data processing methods. Several approaches based on different mechanisms have been developed, such as intermolecular multiple-quantum coherences (iMQCs) [9-17], nutation echoes [1, 18-23], spatial encoding [24-27], coherence transfer echoes [28-31], nuclear Overhauser effect (NOE) [32], reference deconvolution [33, 34], chemical shift imaging (CSI) [35], imaged deconvolution [36], and algorithms based on Fourier synthesis [37].

In this paper, we give a review mainly on the mechanisms and practical implementations of the methodologies based on iMQCs, nutation echoes, and spatial encoding re-

*Address correspondence to this author at the Department of Physics, Xiamen University, Xiamen 361005, China; Tel: +86-592-2180839; Fax: +86-592-2189426; E-mail: shcai@xmu.edu.cn

spectively, and put in perspective for their applicability and efficiency in high-resolution NMR spectroscopy.

2. HIGH-RESOLUTION NMR SPECTRA VIA IMQCS

2.1. Intermolecular Dipole-Dipole Interaction

When a two-pulse sequence separated by a time interval was applied to a highly polarized spin system, multiple spin echoes (MSEs) or iMQCs were observed in the presence of magnetic field gradients [38-40]. Nowadays, the pulse sequences for creating MSEs or iMQCs are mostly based on COSY Revamped with Asymmetric Z-gradient Echo Detection (CRAZED) [39]. They usually contain magnetic field gradient pulses or background magnetic field gradient that modulates the transverse magnetization into a helical structure. There are two superficially quite different frameworks for analyzing the MSEs and iMQCs. In the classical dipolar field framework, the underlying spin physics of related experiments has been described in terms of the distant dipolar field (DDF). The DDF is produced by the spatial modulation of nuclear magnetization from the second radio-frequency (RF) pulse [41-44] and is the integrated effects of dipolar interactions. In this framework, there are only single-quantum coherences (SQCs) during the evolution period of the CRAZED sequence. In the quantum-mechanical density matrix framework, it is suggested that the residual dipolar couplings between distant spins are responsible for the DDF and give rise to iMQCs during the evolution period [39, 40, 45, 46]. Although the classical dipolar field treatment does not refer to the same physical pathways in the CRAZED experiments as the quantum-mechanical treatment, both lead to same quantitative predictions for the signals derived from the pulse sequences [47]. By now an understanding of the effects related to long-range intermolecular dipolar interactions has been developed and the study of these effects is still an active area of research [15, 48-60].

It would be useful to make a qualitative understanding of the origin of the DDF before going into detail. The direct dipole-dipole interaction between any two spins i and j is proportional to $(3 \cos^2 \theta_{ij} - 1)/r_{ij}^3$, where θ_{ij} is the angle between the inter-nuclear vector and the static magnetic field, r_{ij} is the distance between the two spins. For any spin in a liquid sample, its dipole-dipole interactions with nearby spins are averaged away because molecular diffusion makes the isotropic average of $(3 \cos^2 \theta_{ij} - 1)$ go to zero. Thus the net effect of the interactions vanishes. However, it would not be the case for spins at distances longer than molecular diffusion distance on an NMR time scale. Although the dipole-dipole interaction falls off as r_{ij}^{-3} , the total number of spins at a given distance r is proportional to r^2 . Therefore the interaction between one spin and all the spins at a fixed distance r only falls off as $1/r$ [39]. If the spin density is uniform over the sample, the integral of the interactions is zero. If the spatial distribution of spins is made nonuniform, the long-range intermolecular interactions do not cancel out. These interactions between spins were described by the resulting DDF or “dipolar demagnetizing field” as in previous

literature [44]. The combination of RF pulses and gradient pulses or background inhomogeneous fields can create such a nonuniform distribution [39, 40]. Since the term of “dipolar demagnetizing field” cannot accurately describe the related physical processes of MSEs or iMQCs, it is rarely used in recent literature.

In classical model, the DDF $\mathbf{B}_d(\mathbf{r}, t)$ is generally given by

$$\mathbf{B}_d(\mathbf{r}, t) = \frac{\mu_0}{4\pi} \int d^3 r' \frac{1 - 3 \cos^2 \theta_{rr'}}{2 |\mathbf{r} - \mathbf{r}'|^3} [3M_z(\mathbf{r}', t) \hat{\mathbf{z}} - \mathbf{M}(\mathbf{r}', t)], \quad (1)$$

where μ_0 is the vacuum magnetic permeability, $\theta_{rr'}$ is the angle between the static magnetic field and the inter-nuclear vector connecting at position \mathbf{r} and \mathbf{r}' , $\mathbf{M}(\mathbf{r}', t)$ is the magnetization vector in a frame rotating at Larmor frequency, $\hat{\mathbf{z}}$ is the unit vector along the direction of the static magnetic field, and $M_z(\mathbf{r}', t)$ is the magnitude of $\mathbf{M}(\mathbf{r}', t)$ in the $\hat{\mathbf{z}}$ direction [3]. If the magnetization $\mathbf{M}(\mathbf{r}', t)$ varies only along a single direction, as often encountered if gradient pulses are applied along a specific direction s , $\mathbf{B}_d(\mathbf{r}, t)$ can be simplified as

$$\mathbf{B}_d(s, t) = \mu_0 \Delta_s [M_z(s, t) \hat{\mathbf{z}} - \frac{1}{3} \mathbf{M}(s, t)], \quad (2)$$

where $\Delta_s = [3(\hat{s} \cdot \hat{\mathbf{z}})^2 - 1]/2$. The field $\mathbf{B}_d(\mathbf{r}, t)$ is added to the normal form of the Bloch equations, giving an additional contribution $[\mathbf{M}(\mathbf{r}, t) \times \gamma \mathbf{B}_d(\mathbf{r}, t)]$ to $d\mathbf{M}/dt$, where γ is the gyromagnetic ratio.

2.2. Base for High-Resolution Spectra in Inhomogeneous Magnetic Fields

Equation (1) indicates that the DDF is a result of integrated effect coming from all spins. The necessary condition to reduce the non-local DDF into a form that depends on the local magnetization is the existence of a linear field gradient applied along a single direction. A field gradient modulates the resonance frequency of spins as a linear function of space along the field gradient axis, hence the transverse magnetization is wound up into a helix. This helix represents a highly ordered state, but has no net magnetization. It can be subsequently unwound by another field gradient of opposite polarity. The magnitude G and duration δ of the field gradient during a given evolution period τ is kept constant to maintain a fixed half-wavelength of the magnetization helix, or dipolar correlation distance, $d_c = \pi/(\gamma G \delta)$. Adjusting the parameters of the applied field gradient will alter d_c . Typically, intermolecular dipolar interactions are effective in the range of 5-500 μm , which is far smaller than a typical sample size in an NMR experiment. Compared to the scale of inhomogeneity induced by the static magnetic field or susceptibility variation in the sample, the magnetic field within such a short distance scale can be seen as almost homogene-

ous [40, 45, 61]. So it is possible to apply iMQCs to high-resolution NMR spectroscopy in inhomogeneous magnetic fields. Obviously, iMQC-based method would be inherently two-dimensional since the signal has to be transformed to SQCs for detection.

2.3. Applications of iMQCs in High-Resolution NMR Spectroscopy

High-Resolution NMR Spectroscopy Based on iZQCs

Although iMQC signals from high-spin terms have been experimentally detected at high fields [62], the signals of intermolecular zero-quantum coherences (iZQCs), double-quantum coherences (iDQCs), and single-quantum coherences (iSQCs) from two-spin terms in equilibrium density matrix are strongest among any iMQC signals and have found most applications [53, 63-65].

The iZQC signals come from couples of spins with different orientations. The precession frequency of iZQCs in evolution period is

$$\Omega_{iZQC} = \Omega_m(\mathbf{r}') - \Omega_n(\mathbf{r}) = (\omega_m - \omega_n) + \gamma[\Delta B(\mathbf{r}') - \Delta B(\mathbf{r})], \quad (3)$$

where the subscripts m and n represent different spins; ω_m is the frequency offset of spin m in the rotating frame in the absence of magnetic field inhomogeneity; $\Delta B(\mathbf{r})$ is the deviation from the static B_0 field at position \mathbf{r} ; $\Omega_m(\mathbf{r})$ is the frequency offset of spin m at position \mathbf{r} . The deviation of angular frequency from the resonance due to magnetic field inhomogeneity is $\Delta\omega(\mathbf{r}) = \gamma\Delta B(\mathbf{r})$. Since the two coupled spins are spatially close to each other and almost experience a same magnetic field, $\Delta\omega(\mathbf{r}) \approx \Delta\omega(\mathbf{r}')$. Therefore, the iZQC frequency is about $\omega_m - \omega_n$, insensitive to field inhomogeneity. If we acquire a two-dimensional (2D) iZQC spectrum, the projection of spectral peaks onto the indirect dimension is almost free of inhomogeneous broadening. This trait renders the methods based on iZQCs particularly appealing for high-resolution NMR spectroscopy. The HOMOGENIZED (HOMOGENeity ENhancement by Intermolecular ZERo-quantum Detection) sequence proposed by Vathyam and co-workers [14] reveals dramatically enhanced resolution in the indirectly detected dimension of 2D iZQC spectra. It demonstrates the potential of extracting high-resolution NMR information from 2D iZQC spectra in inhomogeneous magnetic fields. Lin and co-workers [15] reported that a composite CPMG-HOMOGENIZED sequence could be adopted to achieve high-resolution spectra in the indirectly detected dimension even in a 25 T electromagnet, whose magnetic field is inherently of low homogeneity and poor stability. Although DDF provides a new and useful way to achieve high-resolution NMR spectra, the intrinsic low signal-to-noise ratio (SNR) of iZQC signals compared to strong conventional SQC signals remains a big technical obstacle. In addition, HOMOGENIZED spectra often suffer from strong t_1 ridge noise at solvent position. Furthermore, the conventional solute signals and solute-solute iZQC signals may decrease the resolution and affect the regeneration of high-resolution one-dimensional (1D) NMR spectra.

In order to overcome above problems, our group proposed a modified pulse sequence, named SEL-HOMOGENIZED, to select only solvent-solute iZQC cross-peaks and greatly suppress the t_1 ridge noise [11]. The second RF pulse in SEL-HOMOGENIZED sequence is selective for solvent spins. Consequently, the solute-solvent iZQC peaks and all trivial cross-peaks originating from solute-solute iZQCs disappear. When the signals from solvent-solute iZQCs achieve maximum, the signal from solvent-solvent iZQCs becomes zero. In addition, a WATERGATE composite pulse $(\pi/2)_{-y,sel} - (\pi)_{y,non-sel} - (\pi/2)_{-y,sel}$ sandwiched between a crusher gradient pair [66] is used for further solvent suppression.

High-Resolution NMR Spectroscopy Based on iDQCs

It has been reported that iDQCs possess features similar to those of iZQCs [56, 67, 68]. Moreover, our previous works show that it is not necessary to use phase cycling or WATERGATE to obtain "pure" iDQC signals since residual SQC signals are greatly suppressed by the iDQC selection gradients, and iDQC signals are approximately 30% stronger than iZQC signals [67]. Therefore, an iDQC sequence (Fig. 1a) named IDEAL (Intermolecular Dipolar-interaction Enhanced All Lines) was designed for high-resolution spectra in inhomogeneous magnetic fields [9]. Similar to the SEL-HOMOGENIZED sequence, the second RF pulse of the IDEAL sequence is selective for solvent spins. The iDQC cross-peaks originating from solute-solute and solute-solvent interactions are eliminated by such selective excitation. The iDQC selection gradients with an area ratio of 1:2 are applied just before and after the second RF pulse to minimize the diffusion-related signal loss. When the effects of relaxation, diffusion, and scalar coupling are neglected, the iDQC cross-peak between I and S spins can be expressed as

$$S_{iDQC} = \frac{1}{3}(\gamma_I M_0^I t_2) M_0^S e^{-i(\Omega_S + \Omega_I)t_1} e^{i\Omega_S t_2} \quad (4)$$

where I indicates solvent and S indicates solute, and M_0 is the equilibrium magnetization. Since the two spins coupled by dipolar interaction are physically close to each other and would experience almost the same local magnetic field, a solvent-solute iDQC peak will have a frequency range of $\Omega_S + \Omega_I = (\omega_S + \omega_I) + 2\Delta\omega(\mathbf{r})$ in the F1 dimension. The corresponding frequency of the solute spins in the F2 dimension ranges in $\Omega_S = \omega_S + \Delta\omega(\mathbf{r})$. Hence, the solvent-solute iDQC cross-peaks will appear as separate streaks along a specific direction $\phi = \arctan 2$ due to the field inhomogeneity, where ϕ is the angle with respect to the F2 axis. Although the ranges of the streaks are susceptible to the field inhomogeneity in both the F1 and F2 dimensions, a projection of the cross-peaks along an axis perpendicular to ϕ regenerates a 1D high-resolution spectrum almost without inhomogeneous broadening. Since the spatial correlation via the DDF of the solvent affects all the spins of solute equally, the relative areas and chemical shifts of the peaks in the 1D projection from a 2D iDQC spectrum are the same as those obtained from a routine high-resolution 1D spectrum. On the

other hand, the scalar coupling is independent of field inhomogeneity in both evolution and detection periods, so the solute spins evolve under scalar couplings in both the F1 and F2 dimensions. The apparent scalar coupling constants in the projection spectrum is 3 times of the conventional ones. This feature may be helpful to obtain refined multiplet patterns in weakly coupled systems, but it may cause distorted multiplet patterns due to spectral peak overlapping in strongly coupled systems.

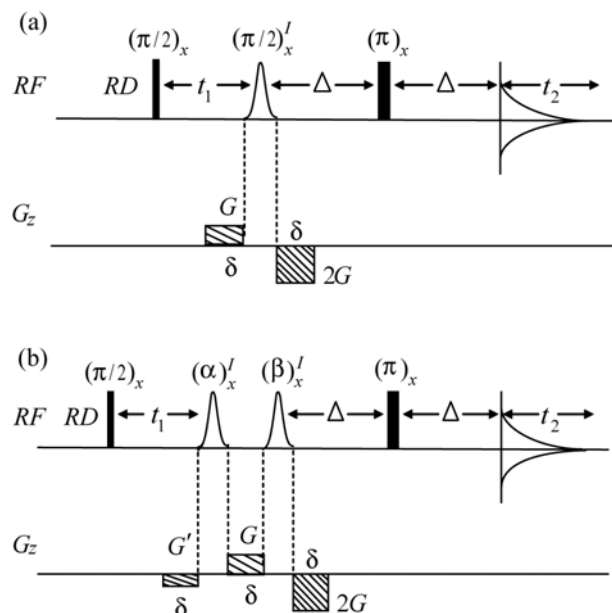


Fig. (1). 2D iMQC pulse sequences: (a) IDEAL sequence; (b) IDQF-HOMOGENIZED sequence. The superscript *I* represents solvent selective. (adapted from [9, 10]).

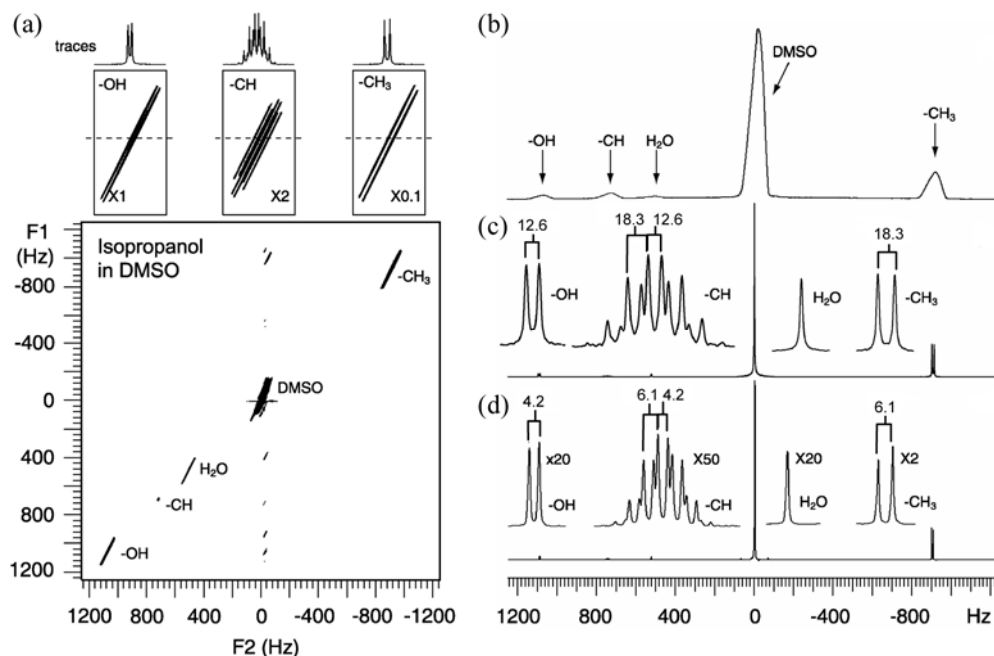


Fig. (2). 500 MHz ^1H NMR spectra of a mixture of 2-propanol and DMSO: (a) IDEAL spectrum in an inhomogeneous field with a linewidth of about 105 Hz. The -OH, -CH, and -CH₃ regions are expanded in both vertical and horizontal directions, above which is the 1D spectra traced along the dashed line; (b) Conventional 1D ^1H spectrum in the same inhomogeneous field; (c) Accumulated projection of the sheared spectrum shown in Fig. (2a); (d) Single-pulse spectrum in a well-shimmed field. (adapted from [9, 10]).

To test the proposed method, a mixture of 2-propanol and dimethylsulfoxide (DMSO) is measured [9]. Fig. (2a) shows the spectrum obtained from the IDEAL sequence. The intermolecular cross-peaks extend along the ϕ direction in the 2D spectrum. The trace indicates that the *J* multiplets are well resolved. To obtain a projection similar to a conventional 1D spectrum, the data matrix needs to shear by $-\pi/2$ along the F1 axis firstly, and then shear by $-\pi/4$ along the F2 axis. After this shearing procedure, a projection along the F1 axis results in a spectrum with inhomogeneous broadening suppressed (Fig. 2c). The linewidth is reduced from 105 to 2 Hz, remarkably similar to the conventional 1D high-resolution ^1H spectrum.

2.4. Improved iMQC Pulse Schemes

In spite of the improvements in spectral resolution, the spectral widths of the F1 and F2 dimensions in the HOMOGENIZED-alike and IDEAL experiments need to be the same, thus long acquisition time (typically several hours) and large data storage space are demanded, which restricts the application of the HOMOGENIZED-alike and IDEAL sequences. Warren group proposed a fast iZQC sequence that enables the acquisition of a 2D iZQC spectrum within a single scan [16]. It can be seen as a superposition of several steps in a HOMOGENIZED experiment with different t_1 values. Enlightened by the *J*-resolved spectral method that refocuses the chemical shift evolution in t_1 period and greatly reduces the spectral width in the F1 dimension, we proposed a fast IDEAL-II method via a “half” delayed acquisition [12]. This method refocuses the double-quantum evolution of solute, leaving the F1 dimension a half t_1 evolution of the solvent and its corresponding inhomogeneous broadening. The reduction in the spectral width of the F1 dimension en-

ables a fast 2D spectral acquisition in one minute. The projected 1D high-resolution spectrum has a scale factor of 3 for the scalar coupling constants.

Except for the efforts to speed up acquisition, spectroscopists also made great efforts on solvent suppression or water suppression (WS). Faber and co-workers presented a zero-quantum selective equivalent of IDEAL, named S90 [13]. It was reported that S90 sequence with two WS modules just before acquisition (S90(WS)²) had best WS efficiency among the existing iZQC sequences. More recently, our group proposed an iZQC sequence named iDQF-HOMOGENIZED, shown in Fig. (1b). The sequence utilizes intermolecular double-quantum filter (iDQF) to suppress solvent signal [10]. Besides iDQF, the use of selective RF pulses allows to select different coherence pathways between solute and solvent, so theoretically not only conventional SQC but also iMQC signals of solvent can be filtered out further by means of coherence selections and optimal flip angles. All these ensure high WS efficiency. The comparison of the solvent signal intensity of a piece of grape sarcocarp from S90, SEL-HOMOGENIZED, S90(WS)², and iDQF-HOMOGENIZED sequences shows that the iDQF-HOMOGENIZED gives best WS efficiency. The two peaks of beta- and alpha-glucose locating at about 0.2 and 0.4 ppm away from the water resonance respectively and completely concealed in the conventional 1D NMR spectrum can be resolved. A weak triplet peak from a methyl group with low concentration at 1.1 ppm also becomes well resolved. Since the apparent *J*-coupling constants are scaled up to 3 times, this sequence is suitable for the study of weakly coupled systems.

3. HIGH-RESOLUTION NMR SPECTRA VIA NUTATION ECHOES

3.1. Situation of *Ex Situ* NMR

NMR experiments are typically performed with samples immersed in a magnet bore shimmed to produce a highly homogeneous static field. However, there are many cases where the sample cannot be placed inside the magnet bore, e.g. the sample size is larger than the magnet bore, or the sample cannot be moved away from its natural environment. In such circumstances, it would be useful if a mobile magnet could be scanned over an otherwise inaccessible object or subject. Efforts to solve this problem lead to crucial development of portable NMR systems [4, 5, 21, 69-71]. These NMR systems have been applied in well-logging, materials science, and biomedicine, etc. [72-75].

The advantage of such *ex situ* analysis is that the limitations of sample size and transportability no longer prevail, but an accompanying handicap is that the magnetic fields are unavoidably spatially inhomogeneous. The field variations are usually orders of magnitude larger than those created by the microscopic structures of the samples to be detected, so chemical shift information cannot be extracted from the NMR spectra. This limits the use of single-sided NMR systems [74, 76-80]. Although the Hahn spin-echo [81] and the Carr-Purcell [82] sequences can remove the inhomogeneous broadening, they also completely refocus the chemical shifts. This situation is changed in 2001 when a novel approach was introduced by Pines and co-workers [18]. This method util-

izes spatially correlated interactions as the mechanism for recovering the chemical shifts, thereby opening a way to high-resolution *ex situ* NMR.

3.2. High-Resolution *Ex Situ* Spectroscopy via Nutation Echoes

For spins with a same chemical shift, different Larmor frequencies $\omega_0(\mathbf{r})$ throughout the sample give rise to progressive dephasing during a free evolution period. At any stage, phase differences due to inhomogeneous magnetic fields can be corrected if a proper position-dependent phase correction is applied. Such a position-dependent phase correction can be accomplished by nutation echo methods, in which RF pulse field $\mathbf{B}_1(\mathbf{r})$ is applied to precisely counteract the phase dispersion originating from the inhomogeneity of static magnetic field $\mathbf{B}_0(\mathbf{r})$ while retaining the modulation due to the chemical shifts. Nutation echoes are generated when $\mathbf{B}_1(\mathbf{r})$ matches $\mathbf{B}_0(\mathbf{r})$ (spatially linear or non-linear correlation) over a region of sample [18, 20, 83, 84]. Nutation echo methods are conceptually different from the iMQC ones. It allows for the detection of a high-resolution spectrum in a single shot.

Nutation Echo Method in Spatially Linear Correlated Magnetic Fields

When $\mathbf{B}_1(\mathbf{r})$ and $\mathbf{B}_0(\mathbf{r})$ are linearly correlated, there exists

$$\frac{d\mathbf{B}_1(\mathbf{r})}{d\mathbf{r}} = k \frac{d\mathbf{B}_0(\mathbf{r})}{d\mathbf{r}}, \quad \mathbf{B}_0(\mathbf{r}) \cdot \mathbf{B}_1(\mathbf{r}) = 0, \quad (5)$$

where the proportionality constant *k* is position-independent. In such case, a single RF pulse $\beta(\mathbf{r})$ is enough to accomplish a position-dependent phase correction. The rotation angle β depends on the local RF strength $\omega_1(\mathbf{r})$. For a fixed pulse length τ , the phase correction at each site is given by $\beta(\mathbf{r}) = \omega_1(\mathbf{r})\tau$. Thus a nutation echo is formed after $t = k\tau$. The measured signal at this point is insensitive to field inhomogeneities but preserves the chemical shift information during time *t*. Note that only half of the signal is recovered. A complete nutation echo can be recovered if the inhomogeneous RF pulse is followed by an ideal $\pi/2$ pulse, which is phase shifted by $\pi/2$ with respect to the RF gradient pulse. Such an ideal $\pi/2$ rotation can be implemented with constant rotation B_1 insensitive composite pulses. Fig. (3a and 3b) show two stroboscopic refocusing pulse sequences using composite *z*-rotation pulses with the form $(\frac{\pi}{2})_{-y} \beta_x (\frac{\pi}{2})_y$ [19]. The inhomogeneous *z*-rotation pulse causes position-dependent phase shift of the transverse magnetization, thus refocusing the dephasing due to the inhomogeneous B_0 field. A train of composite *z*-rotation pulses induces nutation echoes over a region of matched RF pulse and static field gradients. At the same time, stroboscopic acquisition is adopted to acquire data only at echo peaks. The combination of the repeated application of composite *z*-rotation pulses with

stroboscopic acquisition enables direct detection of resolved NMR spectra in inhomogeneous magnetic fields. In the experiments of trans-2-pentenal, the chemical shifts could be resolved when B_0 gradient was 0.12 mT/cm and spectral linewidth reached 2.2 kHz (Fig. 4). However, the scalar coupling multiplet patterns remained masked in the inhomogeneous broadening [18].

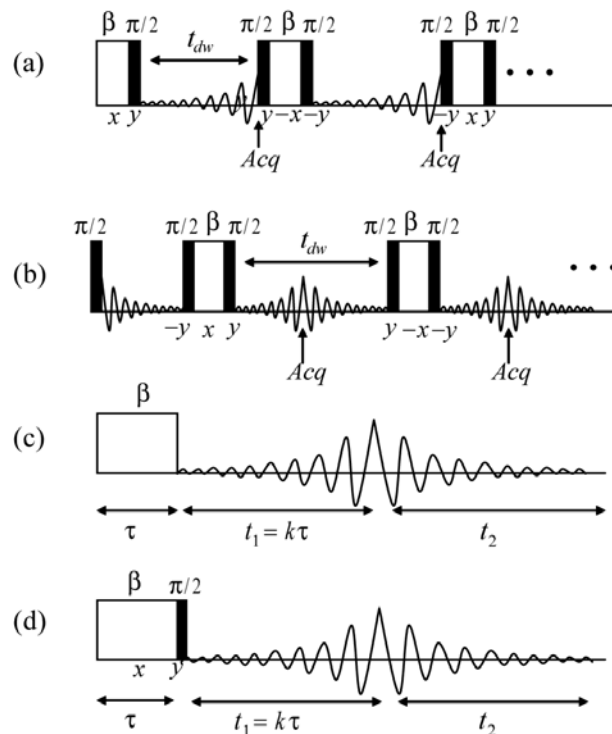


Fig. (3). Some nutation echoes based sequences: (a) and (b) Arrangements of inhomogeneous composite z-rotation pulses for stroboscopic acquisition of resolved spectra; (c) 2D nutation echo sequence in the absence of 90° pulses; (d) 2D nutation echo sequence with full signal recovery. The ideal $\pi/2$ pulses, approximated by constant rotation composite pulses, are depicted in black and inhomogeneous RF pulses are depicted in white (adapted from [19]).

The extension of these principles to multidimensional spectroscopy is straightforward. Based on the concept of nutation echoes in the indirect dimension, a very simple pulse sequence is presented in Fig. (3c) [19], which can yield a depth sensitive 2D NMR spectra with high resolution in the indirect dimension. The pulse sequence consists of one single RF gradient pulse. Instead of a fixed one as in 1D spectroscopy, the duration of the pulse is incremented with t_1 . The acquisition begins at the echo peak. A 1D high-resolution spectrum can be extracted from the resulting 2D spectra by projection onto the F1 dimension. Moreover, a high-resolution 2D spectrum can be obtained when stroboscopic acquisition is adopted to the direct dimension. Using this method, not only chemical shift information, but also the scalar coupling cross-peaks were recovered in the COSY experiment of trans-2-pentenal [19]. Fig. (3d) displays a variation of this pulse sequence, which uses a constant rota-

tion composite $\pi/2$ pulse after the RF gradient pulse and therefore leads to a recovery of the complete signals. Moreover, if the refocusing in the direct dimension is combined with a coherence transfer superimposed on the nutation echo and stroboscopic acquisition, a 2D correlation spectrum can be obtained [18, 19]. A basic 2D nutation echo experiment without delayed acquisition was also suggested for high-resolution spectra in *ex situ* NMR [84]. If B_0 and B_1 fields are perfectly spatially linear correlated within the sample volume, each chemically distinct species would appear as a straight ridge in the final 2D nutation echo spectrum and a high-resolution NMR spectrum can be extracted by either projection or cross section.

In a word, in the case where the correlation of the spatially inhomogeneous RF pulse field and static magnetic field is linear throughout the sample, 1D high-resolution spectra can be obtained either by shearing the 2D nutation echo spectra and taking the projections along the F1 dimension, or by a whole echo acquisition. The residual linewidth in such spectra depends on the quality of the correlation, i.e. on how unique the correspondence between B_0 and B_1 is throughout the sample.

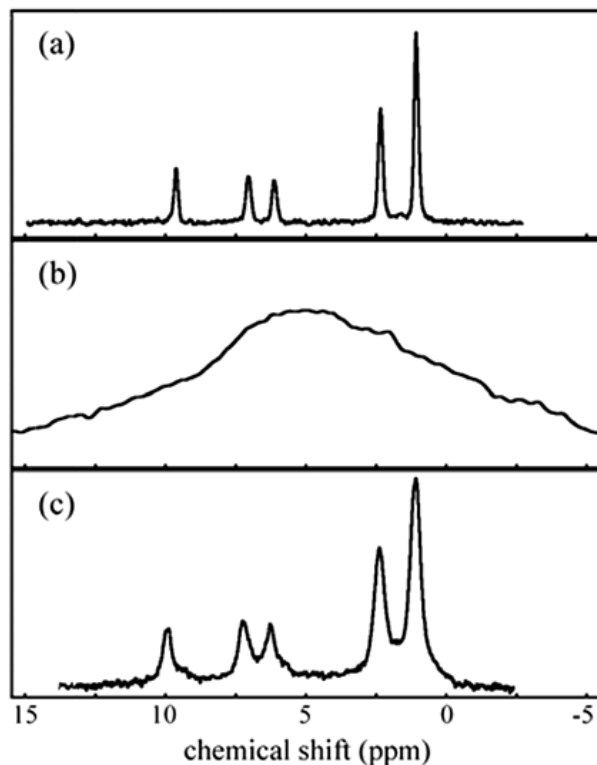


Fig. (4). 179.12 MHz ^1H NMR spectra of trans-2-pentenal acquired with sample attached outside the RF coil. (a) Single-pulse spectrum with linewidth ~ 40 Hz dominated by the intrinsic residual inhomogeneity of the magnetic field; (b) Single-pulse spectrum in the presence of a linear static field gradient of 0.12 mT/cm along the sample axis; (c) Spectrum obtained with the nutation echo sequence in Fig. (3a) in the presence of the same field gradient (adapted from [18]).

Nutation Echo Method in Spatially Non-Linear Correlated Magnetic Fields

In order to gain sensitivity, one needs to work with a maximum sample size in real applications. It means to work with a volume where the B_0 and B_1 fields are correlated in a linear or non-linear way. When the B_0 and B_1 fields are not linearly correlated, the gradient of the static magnetic field is some function of the gradient of the RF field [1]:

$$\frac{dB_0(\mathbf{r})}{d\mathbf{r}} = f \frac{dB_{\text{eff}}(\mathbf{r})}{d\mathbf{r}}, \quad (6)$$

where $B_{\text{eff}}(\mathbf{r})$ is the effective RF field at position \mathbf{r} , whose amplitude can be expressed as $B_{\text{eff}}(\mathbf{r}) = \sqrt{B_1^2(\mathbf{r}) + (B_0(\mathbf{r}) + \delta)^2}$, δ is the chemical shift of each spin species. Compared to the case of spatially linear correlation, the nutation echo experiment in a non-linear case gives a 2D map containing narrow lines that cannot be easily deconvolved or sheared. The ridges are curved rather than straight [20, 84]. However, this does not affect the cross section extraction. The pulse sequence shown in Fig. (3c) is very simple, avoiding sophisticated pulses interleaved with data acquisition. It not only provides spatial resolution in one dimension, but also possesses the great advantage of not requiring a linear correlation between the B_0 and B_1 fields.

Next we give a brief description of the composite and adiabatic z -rotation pulses [23] used to provide refocusing for inhomogeneous magnetic fields.

Composite z -Rotation Pulses

Composite z -rotation pulses, usually composite RF pulses, make magnetization rotate in the xy -plane around z -axis of the rotating frame. Since a composite RF pulse has a net effect of spatially modulating phase shift, it can be used to refocus the effect of different Larmor frequencies in such a way that spins in identical chemical environment give rise to narrow signals with the chemical shifts maintained [18, 85]. The simplest z -rotation pulse has the form $(\frac{\pi}{2})_{-y} \beta_x (\frac{\pi}{2})_y$, which acts as an β -flip-angle z -rotation pulse [1]. The two $\frac{\pi}{2}$ RF pulses are spatially evenly-excited pulses, while the RF pulse β is a spatially inhomogeneous pulse. If the B_0 and B_1 gradients are linearly correlated, the composite pulse would compensate the development of magnetization under the influence of the inhomogeneous external magnetic field. The inhomogeneity is refocused to form a nutation echo after a time interval τ [86-88]. The amplitude of the echo is modulated by the chemical shifts [18].

New compensated composite pulses have been developed in order to satisfy the need for robustness and control over the correlation range of the pulses [22]. They have been shown to be efficient in the presence of high field gradients expected in real *ex situ* experiments. Frequency selectivity is a significant advantage of such pulses. Therefore, they can

be used to limit the sample of interest only to the region where good spatial correlation takes place (narrowband property), thus enhancing the spectral resolution. The inherent efficiency in terms of RF power and short length also makes them possible to refocus the inhomogeneous interaction in a rate fast enough to avoid interference or dephasing of the transverse coherences due to molecular diffusion.

Adiabatic z -Rotation Pulses

Adiabatic pulses [23, 89, 90] are RF pulses which are swept slowly (adiabatically) so that the bulk magnetization vector \mathbf{M} remained approximately collinear with effective field \mathbf{B}_{eff} . If \mathbf{M} is perpendicular to \mathbf{B}_{eff} during the adiabatic passage, a variable flip angle is produced, since different isochromats evolve at different rates about \mathbf{B}_{eff} . The net rotation axis for these perpendicular components of \mathbf{M} is dependent on the initial orientation of \mathbf{M} . Compared to composite pulses, adiabatic pulses generally offer greater combined immunity to B_1 inhomogeneities and resonance offsets for a given amount of RF power. Thus they have broadband property and can operate over a much larger RF and offset ranges [23]. This renders them more robust to manipulate a large portion of the sample than composite pulses and yield better SNR. Adiabatic pulses have found applications in excitation, inversion and decoupling. However, adiabatic z -rotation pulses were only presented and applied to *ex situ* NMR recently [23]. Such z -rotation pulses adopted two full-passage adiabatic pulses applied immediately one after the other. The correlation between the RF coils and the magnet dictates the pattern of the pulses. The first passage induces a phase modulation of the transverse magnetization that strongly depends on the local value of the RF field. The second passage reverses the sense of the modulation. The net accumulated phase cancel the B_0 inhomogeneities. Since the adiabatic pulses are comparatively long, the process may be inadequate for systems with short relaxation times or with a high diffusion coefficient.

The concatenation of two adiabatic pulses contains several degrees of parametric freedom, which can be adjusted for a best correlation between the static magnetic and RF fields. This so-called "active matching" can be performed numerically and even experimentally [1]. Recently, Pines and co-workers put forward an advanced concept "shim pulses" [91], which is corresponding to the role of "shim coils" in a normal high-resolution spectrometer. The shim pulses compensate the imperfection of experimental environments and hardware through a real-time tuning of the adjustable parameters of applied static field gradients and adiabatic RF pulses for high-resolution NMR and MRI. It is a promising idea for high-resolution *ex situ* NMR.

4. HIGH-RESOLUTION NMR SPECTRA VIA SPATIAL ENCODING AND PHASE CORRECTION

Spatial encoding of NMR interactions is another option for achieving narrow lines in the presence of B_0 inhomogeneities. Instead of the usual Ωt phase modulation underlying Fourier transform (FT) NMR, spatial encoding monitors spin evolution by a spatial modulation of the Ω interactions, Ω is

the internal frequency stemming for instance from chemical shift or scalar coupling [92]. Spatial encoding method can operate on a single-scan basis and make direct phase compensation for dephasing caused by inhomogeneous magnetic fields possessing arbitrary spatial dependencies [93, 94]. It opens up new avenues towards the removal of magnetic field inhomogeneities.

The principle of spatial encoding can be understood by a simple example. Assume that a train of frequency-shifted RF pulses and a longitudinal field gradient G_e are applied to the sample. This partitions the sample into N_1 independent spin packets positioned at z_j coordinates, whose evolution frequencies become encoded along the geometry of the field gradient according to $\phi(z_j) = C\Omega(z_j - z_{N_1})$, $j = 1, \dots, N_1$, $C \approx 2T_p G_e / \Delta O$. Here T_p is the duration of G_e , $\Delta O = |O_j - O_{j+1}|$ is the offset increment of excitation pulses. The resulting winding of magnetizations can be uncoiled by an acquisition field gradient G_a , which reveals the evolution frequencies by creating distinct echoes whenever $k = \int G_a(t') dt' = -C\Omega$. This spatial decoding process can last arbitrarily short acquisition time T_a . This enables the acquisition of numerous spectra within the transverse relaxation decay of the spins, thus enhancing experimental sensitivity. In inhomogeneous field with uniaxial ΔB_0 , each of the spatial elements involved in the Ω encoding precesses with a phase depending both on the internal interactions being sought as well as on the artificial ΔB_0 . The distortions imparted into the helical magnetization pattern are given by additional $\Delta\phi(z_j) \approx C \cdot \Delta B_0(z_j) \cdot (z_j - z_{N_1})$ precession phases. These distortions can be accounted for by adding proper phase corrections to the spatially encoding RF pulses. To implement such compensation, the ΔB_0 experienced by spin packets as a function of their z positions must be determined in advance.

A number of routes exploiting the compensation of B_0 inhomogeneities by RF fields have been depicted by Frydman and co-workers recently [24, 25]. These include indirect-domain spatial encoding compensation, direct-domain spatial encoding compensation, and multi-scan 2D compensation approaches.

4.1. Indirect-Domain Spatially-Encoded Single-Scan Strategies

Both discrete and continuous pulse sequences have been proposed for achieving spatial encoding underlying single-scan nD NMR [27, 93, 95-97]. In the discrete encoding mode (Fig. 5a), N_1 discrete excitation pulses trigger the evolution of spins at different positions $\{r_j\}_{j=1, 2, \dots, N_1}$ over a series of incremental times $t_1(r_j) = C(r_j - r_{N_1})$. In order to implement such spatially-selective excitations a suitably refocused encoding gradient G_e is activated, and the offsets $\{O_j\}_{j=1, 2, \dots, N_1}$ of the excitation pulses are regularly spread

between the $\pm\gamma G_e L / 2$ frequency bounds dictated by the sample length L [24]. The overall position-dependent phase accumulated by spins following such discrete spatial encoding process is $\phi_e(r_j) = C\Omega(r_j - r_{N_1})$, $j = 1, \dots, N_1$. In the presence of field inhomogeneities, individual positions r_i are addressed by the RF excitation pulses according to $O(r_i) = \gamma G_e r_i + \Omega_{inh}(r_i)$, and the overall phase evolution at position z_j is

$$\phi_e(r_j) = C \left[\Omega + \Omega_{inh}(r_j) \right] \times (r_j - r_{N_1}), \quad (7)$$

where $\Omega_{inh} = \Delta B / \gamma$. With regard to the discrete option, Frydman group suggested a route with a suitable train of the refocusing RF pulses whose phases $\phi_{RF}(r_j)$ compensate for the additional phase shifts incurred by the field inhomogeneities, and the overall evolution phase is

$$\phi_e(r_j) = C \left[\Omega + \Omega_{inh}(r_j) \right] \times (r_j - r_{N_1}) + \phi_{RF}(r_j). \quad (8)$$

Setting the phases of the RF pulses to $\phi_{RF}(r_j) = -C\Omega_{inh}(r_j) \times (r_j - r_{N_1})$ will remove the effects of the field inhomogeneities, while keep the Ω evolution to be measured [25].

A number of alternatives to this discrete encoding have been proposed. As an example we discuss a $\pi/2 - \pi/2$ combination (Fig. 5b), an approach in which adiabatic swept RF pulses are applied twice: first over an initial time t_p^+ to effect a progressive excitation of the spins, and then over a final time t_p^- to implement a regressive storage of the transverse evolution. These pulses result an amplitude modulation of stored magnetizations. In homogeneous field, the offset of these two chirped pulses is swept over the relevant $|\gamma G_e L|$ frequency intervals at a constant rate $R \approx 2\gamma G_e L / t_1^{\max}$ during equal periods $t_p^+ = t_p^- = t_1^{\max} / 2$. The RF intensity is set as $\gamma B_1 \approx 0.25\sqrt{R}$ to achieve identical $\pi/2$ nutations. In inhomogeneous field, the two pulses act on spins progressively at times $\tau^\pm(r)$ when their RF offsets match $O^\pm[\tau^\pm(r)] = \omega^\pm(r) = \gamma G_e^\pm r + \Omega_{inh}(r)$. The overall phase that gets evolved by the spins' magnetizations will then be given by

$$\phi_e(r) = [t_p^+ - \tau^+(r)] \omega^+(r) + \tau^-(r) \omega^-(r) + \phi_{RF}[\tau^+(r)] - \phi_{RF}[\tau^-(r)], \quad (9)$$

where

$$\phi_{RF}[\tau^\pm(r)] = \int_0^{\tau^\pm(r)} O^\pm(\tau') d\tau' \quad (10)$$

To remove the inhomogeneous field, it is needed to deprive the spatial dependence of $\phi_e(r)$, i.e.

$$\frac{d\phi_e(r)}{dr} = 0 \quad (11)$$

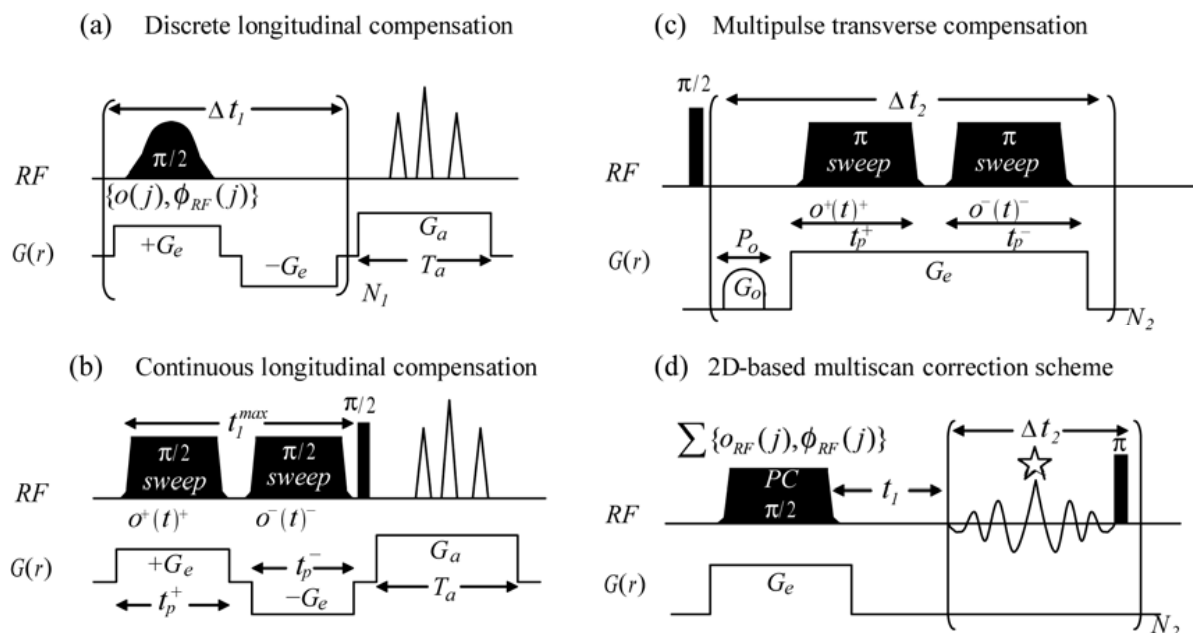


Fig. (5). Spatially-encoded strategies capable of yielding high-resolution spectra with compensated field inhomogeneities by means of the combined application of shaped RF pulses and refocused field gradients. (a) Indirect-domain discrete spatially-encoded scheme; (b) Indirect-domain continuous spatially-encoded scheme; (c) Direct-domain spatially-encoded scheme; (d) 2D multiscan spatially-encoded scheme. (adapted from [24]).

Furthermore, the overall free evolution time t_1 must fulfill

$$t_1(r) = [t_p^+ - \tau^+(r)] + \tau^-(r) = C(r_0 - r), \quad (12)$$

with $C = t_1^{\max} / L$ and $r_0 = -L/2$. From Eqs. (9)-(12), the expressions of times $\tau^\pm(r)$ can be obtained, which can be inverted into $r(\tau^\pm)$ for the frequency sweep profiles of the encoding pulses. The durations of the swept pulses t_p^+ , t_p^- cease to be identical in inhomogeneous field.

4.2. Direct-Domain Spatially-Encoded Single-Scan Strategies

It has been explained how inhomogeneous field is removed in the indirect-domain. In fact, inhomogeneous field can also be removed in the acquisition period through spatially-dependent z-rotations. A simple way to impart this kind of rotations is shown in Fig. (5c), where a pair of frequency-chirped $\pi - \pi$ pulses spanning the shortest possible times t_π^+ , t_π^- act in the presence of pulsed gradients G_e and in-between the signal digitization. Since each π pulse reverses the effects of the chemical shifts, the chemical shifts in the resulting spectrum are scaled by a factor $\frac{t_\pi^+ + t_\pi^-}{t_\pi^+ + t_\pi^- + \Delta t_2}$. This approach compensates the inhomogeneities N_2 times that equals the number of digitized points, imparting at every instance a correction corresponding to the evolution time Δt_2 . The correction strategy is similar to the

one described for Fig. (5b). The overall phase evolved during the course of each transverse dwelling time Δt_2 is

$$\phi_e(r) = \phi_\pi^-(r) - \phi_\pi^+(r) + \phi_{inh}^-(r) + \phi_{inh}^+(r). \quad (13)$$

Here

$$\phi_\pi^\pm(r) = -\tau^\pm(r)\omega^\pm(r) + 2\phi_{RF}^\pm[\tau^\pm(r)] + [t_\pi^\pm - \tau_\pi^\pm(r)]\omega^\pm(r), \quad (14)$$

where $\phi_{inh}^\pm(r) = \left[\frac{\Delta t_2}{2} - t_\pi^\pm \right] \Omega_{inh}^\pm(r)$. Eq. (14) denotes the

phase evolutions the two consecutive π inversions impart in the rotating frame.

To compensate ϕ_{inh}^\pm , Frydman group chose to tailor the offset-driven ϕ_{RF}^\pm terms in Eq. (14). Assume that the gradient shapes are equal over the course of the π pulses, $\omega^\pm(r) = \gamma G_e r + \Omega_{inh}^\pm(r)$. In this case, a small additional gradient pulse in the form of $k_o = G_o P_o$ is added to enable the presence of a period of free evolution, where G_o is the strength of the gradient and P_o is its duration. This adds an overall additional phase $k_o r$. The inhomogeneity-compensated evolution condition then becomes $\frac{d\phi_e(r)}{dr} = k_o$. From this evolution condition and the $\tau^\pm(r)$ boundary conditions, one can obtain the offset frequency shapes $O[r(\tau^\pm)]$. The amplitudes of the resulting RF sweeps also need to be tailored to fulfill the adiabatic demand of π inversion.

To evaluate the refocusing performance of the above inhomogeneity compensation approaches, a series of ^1H NMR experiments of an n-butylchloride/ CDCl_3 solution were carried out on 500 MHz spectrometer [24]. Some results are shown in Fig. (6). The magnetic field was deliberately deshimmmed to produce a uniaxial inhomogeneity. The 1D spectrum acquired in such field is shown in Fig. (6a). The spectral peaks are broadened, so chemical shifts and J couplings cannot be resolved. When the longitudinal correction scheme illustrated in Fig. (5b) was utilized, the linewidth of the spectral peaks was reduced to about 30 Hz, sufficient for the resolution of chemical shifts, yet not sufficient for the resolution of J couplings (Fig. 6b). Similar result was obtained for the scheme shown in Fig. (5a) [25]. When the transverse correction scheme of Fig. (5c) was applied, the linewidth of the spectral peaks was reduced to about 4 Hz (Fig. 6c), allowing the resolution of J couplings. However, due to the scaling of the apparent chemical shifts, the spectrum appeared as that recorded at 75 MHz spectrometer, rather than 500 MHz spectrometer. This influences the line shapes of the peaks close to each other and the resolution of chemical shifts.

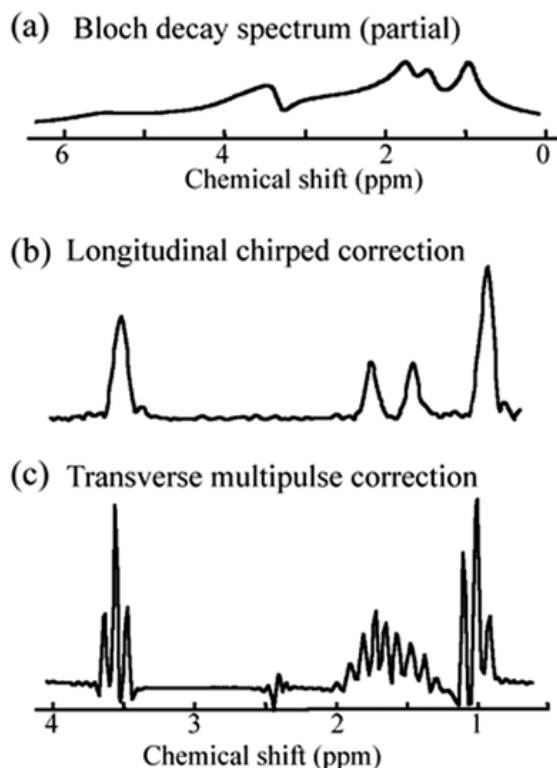


Fig. (6). 500 MHz ^1H NMR spectrum of an n-butylchloride/ CDCl_3 solution to demonstrate the performance of the single-scan schemes to compensate for 1D field inhomogeneities. (a) Artificially broadened spectrum obtained following a single $\pi/2$ pulse excitation; (b) Result from Fig. (5b); (c) Result from Fig. (5c) (adapted from [24]).

The indirect- and direct-domain strategies refocus inhomogeneities in a complementary way: one refocuses inhomogeneities along the indirect t_1 evolution domain, while the other in-between Δt_2 direct-domain dwelling times. Therefore, it is natural to integrate them to explore new opportunities towards the acquisition of 2D NMR spectra in

inhomogeneous magnetic fields. The feasibility has been validated by testing experiments [24].

4.3. Extensions to Multiple-Scan Strategies

All the spatially-encoded strategies mentioned above have their own limitations. The main limitation of the indirect-domain inhomogeneous field compensation approach is its low sensitivity. In addition, the inhomogeneity is not compensated during acquisition period. For the direct-domain compensation approach, the main drawback stems from the substantial scaling of chemical shifts, which make the approach possibly not suitable for the chemical shift-based applications, such as low field MR spectroscopy. To overcome the issues of sensitivity and chemical shifts scaling in these two methods, Frydman group proposed an approach combining the single-instant nature of the spatially encoded compensation principle with the classical scheme of 2D NMR, as shown in Fig. (5d). In such scenario, the inhomogeneities acting over the course of the indirect domain are compensated at the time of excitation by a suitable polychromatic pulse. This pulse acts in a spatially-selective manner with the help of a strong magnetic field gradient. For each t_1 increment, the phases of the N individual components making the polychromatic excitation pulse are set according to

$$[\phi_{RF}]_i = -O(r_i)\tau_p - t_1\Omega_{inh}(r_i), \quad i = 1, \dots, N, \quad (15)$$

where τ_p is the duration of the polychromatic pulse and $\{O(r_i) = \gamma G_e r_i + \Omega_{inh}(r_i)\}_{i=1, \dots, N}$ are the N basic frequency elements of the polychromatic pulse. The position-dependent evolution phases introduced by the excitation gradient and the $\Omega_{inh}(r)$ distribution would cancel out at the culmination of the indirect-domain evolution period, enabling a high-resolution signal to be sampled. Repeating the procedure a suitable number of t_1 increments would then yield a conventional high-resolution time-domain signal when viewed along the indirect domain. Since no ancillary field gradients are required in the acquisition period, no extra sensitivity loss will occur, and since τ_p can be greatly smaller than t_1^{\max} , no significant scaling of chemical shifts will result.

5. OTHER HIGH-RESOLUTION NMR METHODOLOGIES

Besides the above three kinds of methods, there are many other pulse sequences and data processing methods aimed at recovering spectral information from inhomogeneous broadening, as mentioned in Section 1. Here we give a brief description.

Coherence transfer echo is one kind of echo occurring when coherence is transferred from one transition to another between defocusing and refocusing. The two involved transitions can happen on heteronuclei or different quantum coherence orders. As a special case, total spin coherence transfer echo spectroscopy (TSCTES) uses the property that the transition between two states of a maximum total coherence order is intrinsically insensitive to inhomogeneous magnetic

fields, while sensitive to chemical shift differences and scalar couplings [29, 31]. This technique excites only coupled spin systems, and uncoupled spins are not excited. Therefore, the peaks of isolated spins or subsystems will be lost in the spectra. In heteronuclear transfer echoes, the evolution of one nuclear species under the inhomogeneous field is refocused after a coherence transfer to a second species. The second nucleus behaves as a probe for the local environment of its neighbor. This method has been applied successfully to amorphous solids to get high resolution spectra even in the presence of a distribution of isotropic chemical shifts [30].

A high-resolution NMR method via intermolecular NOE was suggested by Balbach and co-workers [32]. Similar to iMQC methods, an approximation $\Delta B(\mathbf{r}) = \Delta B(\mathbf{r}')$ can be made for solvent spin at \mathbf{r} and solute spin at \mathbf{r}' with short-range dipolar interactions. Therefore, the NOESY cross-peaks display like streaks inclined at a specific angle and 1D high-resolution spectra can be obtained via cross section or projection. However, the intensities of the cross-peaks in a NOESY spectrum are greatly dependent on cross relaxation rate, which is largely decided by spatial conformation of solute molecules. Thus the signals of the solute spins with low cross relaxation rates will be too weak to obtain good SNR, and the signal intensities weighted by cross relaxation rates will not fulfill the demand for quantification, such as relative peak areas.

Reference deconvolution is a post-processing technique that uses the shape of a single resonance line to measure the actual frequency distribution produced by a small-scale local B_0 inhomogeneity and then deconvolves this distribution from the whole spectrum [33, 98]. The pity is that a significant improvement in spectral linewidth exacts a penalty in SNR and lineshape.

The CSI method is based on the simple fact that the variation of the magnetic field within a voxel is much smaller than that across the whole sample volume. When voxel spectra are realigned, a spectrum with much narrower lines compared to the total volume 1D spectrum may be obtained [35]. The shortage of the CSI method is that time consuming is usually required since many phase-encoding steps should be applied to achieve spatial resolution. Besides, the sensitivity loss, which is proportional to the spatial resolution, also restricts the application of the CSI method.

Imaged deconvolution is a compromise between pure reference deconvolution and pure spectroscopic imaging. Reference deconvolution does not work in the case of large line broadening, whereas spectroscopic imaging like CSI places impractical demands on both hardware and experimental time. Imaged deconvolution method finds the optimal compromise between the two methods to render the acquisition of high-resolution spectra in grossly inhomogeneous magnetic fields possible [99].

The Fourier decompositions and pulse sequence design algorithms use Fourier decompositions to design RF pulses and time-varying linear gradients in three dimensions [37]. The designed pulse sequences can be used to precompensate the phase differences of spins at different spatial locations due to inhomogeneous magnetic fields. The problem is that

the sequences derived from the algorithms maybe long (in terms of time) and some signals will be small and even disappear since the relaxation effects are neglected in the treatment.

CONCLUSION

The high-resolution NMR methodologies based on iMQCs, nutation echoes and spatial encoding were reviewed. These methodologies have been theoretically and experimentally proven to be useful to retain high-resolution NMR spectra in inhomogeneous magnetic fields. Taking advantage of each unique property, different methods can be applied to different situations.

In *in vivo* and *in situ* NMR spectroscopy, the magnetic environments are often inhomogeneous. Line broadening due to magnetic susceptibility gradients results in severe problems with peak overlapping. Moreover, solvent peaks are usually intense in biochemical samples, which may conceal solute signals and produce a broad baseline. By means of intermolecular long-range dipolar interactions, the iMQC methods can be used to achieve 1D high-resolution NMR spectra in inhomogeneous magnetic fields with efficient solvent suppression. The spectra can provide information of chemical shifts, scalar couplings, multiplet patterns and relative peak areas, all of which are extremely important for analyzing molecular structures and dynamics. The fundamental requirements of the iMQC methods are that the dipole-coupled molecules are intermingled on a microscopic scale and the solvent has a single resonance with large nuclear magnetization. Potentials of the high-resolution iMQC methods have been demonstrated [10, 16, 17, 100-105], but their intrinsic low SNR usually becomes an obstacle for their implementation. Improved experimental conditions such as higher magnetic field and receiver sensitivity will result in more efficient acquisition and significantly better SNR.

Utilizing the property of matching RF gradients and static field gradients, the methods based on nutation echoes offer an efficient way to recover chemical shift information in the presence of inhomogeneous magnetic fields for *ex situ* situations. Compared to the iMQC methods which adapt to slight and moderate inhomogeneous magnetic fields, nutation echo methods are efficient even in extremely large field inhomogeneities. This makes it possible for single-sided portable magnetic resonance system to be used in high-resolution *ex situ* NMR experiments. However, this method can only provide information of chemical shifts. The scalar coupling multiplet patterns cannot be obtained. Furthermore, there is still a lot of work to do with the magnet and the RF coil design to successfully apply this method to actual *ex situ* situations. Large gradients and/or imperfect non-linear field correlations are issues that should be taken into account during the initial stages of the design of high-resolution open NMR systems. Applications in the fields such as biomedical diagnostics and food analysis would undoubtedly benefit from further development in the technology.

Based on the theory of spatial encoding, a series of single- and multiple-scan compensation approaches have been proposed to retain high-resolution NMR spectroscopy in inhomogeneous magnetic fields. The single-scan approaches have obvious speed advantage, while the sensitivity or reso-

lution is sacrificed. Therefore they are not suitable for low-sensitivity and low-field cases. The multi-scan alternative combines spatially-encoded compensation with traditional 2D NMR approach to dispose of the poor sensitivity and scaled spectral information the single-scan methods have. It is particularly useful in scenarios characterized by relatively high heterogeneities, limited shimming capabilities and relatively low magnetic fields where chemical shift displacements are at a premium. The greatest challenge of the spatial encoding methods is the extension of inhomogeneous field compensation from one spatial dimension to three.

Although different mechanisms make different methods suitable for different situation, there are not definitely different domains in application. They complement each other and contribute together to high-resolution NMR spectroscopy. They will be further refined and expanded driven by a wealth of new applications in NMR, and combinations of different approaches are likely to produce better results.

ACKNOWLEDGEMENTS

This work was partially supported by the National Natural Science Foundation of China (Nos. 10575085 and 20573084), Natural Science Foundation of Fujian Province of China (No. 2008J0028), and NCET of Ministry of Education of China.

REFERENCES

- [1] Sakellariou, D.; Meriles, C.A.; Pines, A. Advances in *ex-situ* nuclear magnetic resonance. *C. R. Phys.*, **2004**, *5*, 337-47.
- [2] Gan, Z.; Kwak, H.T.; Bird, M.; Cross, T.; Gor'kov, P.; Brey, W.; Shetty, K. High-field NMR using resistive and hybrid magnets. *J. Magn. Reson.*, **2008**, *191*, 135-40.
- [3] Wehler, T.; Westman, J. Magic angle spinning NMR: A valuable tool for monitoring the progress of reactions in solid phase synthesis. *Tetrahedron Lett.*, **1996**, *37*, 4771-74.
- [4] Perlo, J.; Casanova, F.; Blümich, B. *Ex situ* NMR in highly homogeneous fields: ¹H spectroscopy. *Science*, **2007**, *315*, 1110-12.
- [5] Blümich, B.; Perlo, J.; Casanova, F. Mobile single-sided NMR. *Prog. Nucl. Magn. Reson. Spectrosc.*, **2008**, *52*, 197-269.
- [6] Ungersma, S.E.; Xu, H.; Chronik, B.A.; Scott, G.C.; Macovski, A.; Conolly, S.M. Shim design using a linear programming algorithm. *Magn. Reson. Med.*, **2004**, *52*, 619-27.
- [7] Brideson, M.A.; Forbes, L.K.; Crozier, S. Determining complicated winding patterns for shim coils using stream functions and the target-field method. *Concepts Magn. Reson.*, **2002**, *14*, 9-18.
- [8] Juchem, C.; Muller-Bierl, B.; Schick, F.; Logothetis, N.K.; Pfeuffer, J. Combined passive and active shimming for *in vivo* MR spectroscopy at high magnetic fields. *J. Magn. Reson.*, **2006**, *183*, 278-89.
- [9] Chen, Z.; Chen, Z.W.; Zhong, J.H. High-resolution NMR spectra in inhomogeneous fields via IDEAL (Intermolecular Dipolar-interaction Enhanced All Lines) method. *J. Am. Chem. Soc.*, **2004**, *126*, 446-47.
- [10] Chen, X.; Lin, M.J.; Chen, Z.; Cai, S.H.; Zhong, J.H. High-resolution intermolecular zero-quantum coherence spectroscopy under inhomogeneous fields with effective solvent suppression. *Phys. Chem. Chem. Phys.*, **2007**, *9*, 6231-40.
- [11] Chen, Z.; Hou, T.; Chen, Z.W.; Hwang, D.W.; Hwang, L.P. Selective intermolecular zero-quantum coherence in high-resolution NMR under inhomogeneous fields. *Chem. Phys. Lett.*, **2004**, *386*, 200-05.
- [12] Chen, Z.; Chen, Z.W.; Zhong, J.H. IDEAL-II: Improved IDEAL (Intermolecular Dipolar interaction Enhanced All Lines) method for high-resolution MRS in inhomogeneous fields. *Proc. Int. Soc. Mag. Reson. Med.*, **2004**, *11*, 2300.
- [13] Balla, D.; Faber, C. Solvent suppression in liquid state NMR with selective intermolecular zero-quantum coherences. *Chem. Phys. Lett.*, **2004**, *393*, 464-69.
- [14] Vathyam, S.; Lee, S.; Warren, W.S. Homogeneous NMR spectra in inhomogeneous fields. *Science*, **1996**, *272*, 92-96.
- [15] Lin, Y.Y.; Ahn, S.; Murali, N.; Brey, W.; Bowers, C.R.; Warren, W.S. High-resolution, > 1 GHz NMR in unstable magnetic fields. *Phys. Rev. Lett.*, **2000**, *85*, 3732-35.
- [16] Galiana, G.; Branca, R.T.; Warren, W.S. Ultrafast intermolecular zero quantum spectroscopy. *J. Am. Chem. Soc.*, **2005**, *127*, 17574-75.
- [17] Lin, Y.Q.; Chen, Z.; Cai, S.H.; Zhong, J.H. Accurate measurements of small J coupling constants under inhomogeneous fields via intermolecular multiple-quantum coherences. *J. Magn. Reson.*, **2008**, *190*, 298-306.
- [18] Meriles, C.A.; Sakellariou, D.; Heise, H.; Moule, A.J.; Pines, A. Approach to high-resolution *ex situ* NMR spectroscopy. *Science*, **2001**, *293*, 82-85.
- [19] Heise, H.; Sakellariou, D.; Meriles, C.A.; Moule, A.; Pines, A. Two-dimensional high-resolution NMR spectra in matched B₀ and B₁ field gradients. *J. Magn. Reson.*, **2002**, *156*, 146-51.
- [20] Topgaard, D.; Sakellariou, D.; Pines, A. NMR spectroscopy in inhomogeneous B₀ and B₁ fields with non-linear correlation. *J. Magn. Reson.*, **2005**, *175*, 1-10.
- [21] Perlo, J.; Demas, V.; Casanova, F.; Meriles, C.A.; Reimer, J.; Pines, A.; Blümich, B. High-resolution NMR spectroscopy with a portable single-sided sensor. *Science*, **2005**, *308*, 1279.
- [22] Sakellariou, D.; Meriles, C.A.; Moule, A.; Pines, A. Variable rotation composite pulses for high resolution nuclear magnetic resonance using inhomogeneous magnetic and radiofrequency fields. *Chem. Phys. Lett.*, **2002**, *363*, 25-33.
- [23] Meriles, C.A.; Sakellariou, D.; Pines, A. Broadband phase modulation by adiabatic pulses. *J. Magn. Reson.*, **2003**, *164*, 177-81.
- [24] Shapira, B.; Frydman, L. Spatially encoded pulse sequences for the acquisition of high resolution NMR spectra in inhomogeneous fields. *J. Magn. Reson.*, **2006**, *182*, 12-21.
- [25] Shapira, B.; Frydman, L. Spatial encoding and the acquisition of high-resolution NMR spectra in inhomogeneous magnetic fields. *J. Am. Chem. Soc.*, **2004**, *126*, 7184-85.
- [26] Shrot, Y.; Frydman, L. Spatially resolved multidimensional NMR spectroscopy within a single scan. *J. Magn. Reson.*, **2004**, *167*, 42-48.
- [27] Shapira, B.; Shetty, K.; Brey, W.W.; Gan, Z.H.; Frydman, L. Single-scan 2D NMR spectroscopy on a 25 T bitter magnet. *Chem. Phys. Lett.*, **2007**, *442*, 478-82.
- [28] Maudsley, A.A.; Wokaun, A.; Ernst, R.R. Coherence transfer echoes. *Chem. Phys. Lett.*, **1978**, *55*, 9-14.
- [29] Weitekamp, D.P.; Garbow, J.R.; Murdoch, J.B.; Pines, A. High-resolution NMR-spectra in inhomogeneous magnetic-fields: Application of total spin coherence transfer echoes. *J. Am. Chem. Soc.*, **1981**, *103*, 3578-79.
- [30] Sakellariou, D.; Brown, S.P.; Lesage, A.; Hediger, S.; Bardet, M.; Meriles, C.A.; Pines, A.; Emsley, L. High-resolution NMR correlation spectra of disordered solids. *J. Am. Chem. Soc.*, **2003**, *125*, 4376-80.
- [31] Garbow, J.R.; Weitekamp, D.P.; Pines, A. Total spin coherence transfer echo spectroscopy. *J. Chem. Phys.*, **1983**, *79*, 5301-10.
- [32] Balbach, J.J.; Conradi, M.S.; Cistola, D.P.; Tang, C.G.; Garbow, J.R.; Hutton, W.C. High-resolution NMR in inhomogeneous fields. *Chem. Phys. Lett.*, **1997**, *277*, 367-74.
- [33] Morris, G.A.; Barjat, H.; Horne, T.J. Reference deconvolution methods. *Prog. Nucl. Magn. Reson. Spectrosc.*, **1997**, *31*, 197-257.
- [34] Morris, G.A.; Gibbs, A. High-sensitivity, high-resolution NMR in inhomogeneous magnetic-fields. *J. Magn. Reson.*, **1988**, *78*, 594-96.
- [35] Sersa, I.; Macura, S. Spectral resolution enhancement by chemical shift imaging. *Magn. Reson. Imaging*, **2007**, *25*, 250-58.
- [36] Halse, M.E.; Callaghan, P.T. Imaged deconvolution: A method for extracting high-resolution NMR spectra from inhomogeneous fields. *J. Magn. Reson.*, **2007**, *185*, 130-37.
- [37] Pryor, B.; Khaneja, N. Fourier decompositions and pulse sequence design algorithms for nuclear magnetic resonance in inhomogeneous fields. *J. Chem. Phys.*, **2006**, *125*, 194111.
- [38] Bowtell, R.; Bowley, R.M.; Glover, P. Multiple spin echoes in liquids in a high magnetic field. *J. Magn. Reson.*, **1990**, *88*, 643-51.

- [39] Warren, W.S.; Richter, W.; Andreotti, A.H.; Farmer, B.T. Generation of impossible cross-peaks between bulk water and biomolecules in solution NMR. *Science*, **1993**, *262*, 2005-09.
- [40] Lee, S.; Richter, W.; Vathyam, S.; Warren, W.S. Quantum treatment of the effects of dipole-dipole interactions in liquid nuclear magnetic resonance. *J. Chem. Phys.*, **1996**, *105*, 874-900.
- [41] Deville, G.; Bernier, M.; Delrieux, J.M. NMR multiple echoes observed in solid ^3He . *Phys. Rev. B*, **1979**, *19*, 5666-87.
- [42] Jeener, J.; Vlassenbroek, A.; Broekaert, P. Unified derivation of the dipolar field and relaxation terms in the Bloch-Redfield equations of liquid NMR. *J. Chem. Phys.*, **1995**, *103*, 1309-32.
- [43] Vlassenbroek, A.; Jeener, J.; Broekaert, P. Macroscopic and microscopic fields in high-resolution liquid NMR. *J. Magn. Reson.*, **1996**, *118*, 234-46.
- [44] Levitt, M.H. Demagnetization field effects in two-dimensional solution NMR. *Concepts Magn. Reson.*, **1996**, *8*, 77-103.
- [45] He, Q.H.; Richter, W.; Vathyam, S.; Warren, W.S. Intermolecular multiple-quantum coherences and cross correlations in solution nuclear-magnetic-resonance. *J. Chem. Phys.*, **1993**, *98*, 6779-800.
- [46] Warren, W.S.; Lee, S.; Richter, W.; Vathyam, S. Correcting the classical dipolar demagnetizing field in solution NMR. *Chem. Phys. Lett.*, **1995**, *247*, 207-14.
- [47] Jeener, J. Equivalence between the "classical" and the "Warren" approaches for the effects of long range dipolar couplings in liquid nuclear magnetic resonance. *J. Chem. Phys.*, **2000**, *112*, 5091-94.
- [48] Lin, Y.Y.; Lisitz, N.; Ahn, S.D.; Warren, W.S. Resurrection of crushed magnetization and chaotic dynamics in solution NMR spectroscopy. *Science*, **2000**, *290*, 118-21.
- [49] Walls, J.D.; Phoa, F.K.H.; Lin, Y.Y. Spin dynamics at very high spin polarization. *Phys. Rev. B*, **2004**, *70*, 174410.
- [50] Kimmich, R.; Ardelean, I.; Lin, Y.Y.; Ahn, S.; Warren, W.S. Multiple spin echo generation by gradients of the radio frequency amplitude: Two-dimensional nutation spectroscopy and multiple rotary echoes. *J. Chem. Phys.*, **1999**, *111*, 6501-09.
- [51] Zhong, J.H.; Chen, Z.; Zheng, S.K.; Kennedy, S.D. Theoretical and experimental characterization of NMR transverse relaxation process related to intermolecular dipolar interactions. *Chem. Phys. Lett.*, **2001**, *350*, 260-68.
- [52] Wong, C.K.; Kennedy, S.D.; Kwok, E.; Zhong, J.H. Theoretical studies of the effect of the dipolar field in multiple spin-echo sequences with refocusing pulses of finite duration. *J. Magn. Reson.*, **2007**, *185*, 247-58.
- [53] Kennedy, S.D.; Zhong, J.H. Diffusion measurements free of motion artifacts using intermolecular dipole-dipole interactions. *Magn. Reson. Med.*, **2004**, *52*, 1-6.
- [54] Ardelean, I.; Kossel, E.; Kimmich, R. Attenuation of homo- and heteronuclear multiple spin echoes by diffusion. *J. Chem. Phys.*, **2001**, *114*, 8520-29.
- [55] Zhang, H.M.; Lizitsa, N.; Bryant, R.G.; Warren, W.S. Experimental characterization of intermolecular multiple-quantum coherence pumping efficiency in solution NMR. *J. Magn. Reson.*, **2001**, *148*, 200-208.
- [56] Chen, Z.; Chen, Z.W.; Zhong, J.H. Quantitative characterization of intermolecular dipolar interactions of two-component systems in solution nuclear magnetic resonance. *J. Chem. Phys.*, **2001**, *115*, 10769-79.
- [57] Chen, Z.; Zhong, J.H. Unconventional diffusion behaviors of intermolecular multiple-quantum coherences in nuclear magnetic resonance. *J. Chem. Phys.*, **2001**, *114*, 5642-53.
- [58] Chen, Z.; Chen, Z.W.; Zhong, J.H. Observation and characterization of intermolecular homonuclear single-quantum coherences in liquid nuclear magnetic resonance. *J. Chem. Phys.*, **2002**, *117*, 8426-35.
- [59] Zhu, X.Q.; Cai, C.B.; Chen, Z.; Zhong, J.H. Multiplet patterns due to co-existing intermolecular dipolar and intramolecular scalar couplings in liquid nuclear magnetic resonance. *Chin. Phys.*, **2005**, *14*, 516-23.
- [60] Zheng, B.W.; Chen, Z.; Cai, S.H.; Zhong, J.H.; Ye, C.H. Theoretical formalism and experimental verification of line shapes of NMR intermolecular multiple-quantum coherence spectra. *J. Chem. Phys.*, **2005**, *123*, 074317.
- [61] Bowtell, R.; Robyr, P. Structural investigations with the dipolar demagnetization field in solution NMR. *Phys. Rev. Lett.*, **1996**, *76*, 4971-74.
- [62] Chen, Z.; Chen, Z.W.; Hwang, D.W.; Zhong, J.H.; Hwang, L.P. Separation and characterization of different signals from intermolecular three-spin orders in solution NMR. *J. Magn. Reson.*, **2004**, *171*, 244-52.
- [63] Zhong, J.H.; Chen, Z.; Kwok, W.E.; Kennedy, S.; You, Z.Y. Optimization of blood oxygenation level-dependent sensitivity in magnetic resonance imaging using intermolecular double-quantum coherence. *J. Magn. Reson. Imaging*, **2002**, *16*, 733-40.
- [64] Marques, J.P.; Bowtell, R. Optimizing the sequence parameters for double-quantum CRAZED imaging. *Magn. Reson. Med.*, **2004**, *51*, 148-57.
- [65] Balla, D.Z.; Faber, C. Localized intermolecular zero-quantum coherence spectroscopy *in vivo*. *Concepts Magn. Reson. Part A*, **2008**, *32A*, 117-33.
- [66] Price, W.S.; Elwinger, F.; Vigouroux, C.; Stilbs, P. PGSE-WATERGATE, a new tool for NMR diffusion-based studies of ligand-macromolecule binding. *Magn. Reson. Chem.*, **2002**, *40*, 391-95.
- [67] Zhong, J.H.; Chen, Z.; Kwok, E. *In vivo* intermolecular double-quantum imaging on a clinical 1.5 T MR scanner. *Magn. Reson. Med.*, **2000**, *43*, 335-41.
- [68] Mori, S.; Hurd, R.E.; van Zijl, P.C.M. Imaging of shifted stimulated echoes and multiple spin echoes. *Magn. Reson. Med.*, **1997**, *37*, 336-40.
- [69] Kleinberg, R.L.; Sezginer, A.; Griffin, D.D. Novel NMR apparatus for investigating an external sample. *J. Magn. Reson.*, **1992**, *97*, 466-85.
- [70] Eidmann, G.; Savelsberg, R.; Blumler, P.; Blümich, B. The NMR MOUSE, a mobile universal surface explorer. *J. Magn. Reson.*, **1996**, *122*, 104-09.
- [71] Demas, V.; Sakellariou, D.; Meriles, C.A.; Han, S.; Reimer, J.; Pines, A. Three-dimensional phase-encoded chemical shift MRI in the presence of inhomogeneous fields. *Proc. Natl. Acad. Sci. USA*, **2004**, *101*, 8845-47.
- [72] Hurlimann, M.D.; Griffin, D.D. Spin dynamics of Carr-Purcell-Meiboom-Gill-like sequences in grossly inhomogeneous B_0 and B_1 fields and application to NMR well logging. *J. Magn. Reson.*, **2000**, *143*, 120-35.
- [73] Zimmer, G.; Guthausen, A.; Blümich, B. Characterization of cross-link density in technical elastomers by the NMR-MOUSE. *Solid State Nucl. Magn. Reson.*, **1998**, *12*, 183-90.
- [74] Haken, R.; Blümich, B. Anisotropy in tendon investigated *in vivo* by a portable NMR scanner, the NMR-MOUSE. *J. Magn. Reson.*, **2000**, *144*, 195-99.
- [75] Ruhi, F.J.; Boni, T.; Perlo, J.; Casanova, F.; Baias, M.; Egarter, E.; Blümich, B. Non-invasive spatial tissue discrimination in ancient mummies and bones *in situ* by portable nuclear magnetic resonance. *J. Cult. Herit.*, **2007**, *8*, 257-63.
- [76] Wiesmath, A.; Filip, C.; Demco, D.E.; Blümich, B. Double-quantum-filtered NMR signals in inhomogeneous magnetic fields. *J. Magn. Reson.*, **2001**, *149*, 258-63.
- [77] Balibanu, F.; Hailu, K.; Eymael, R.; Demco, D.E.; Blümich, B. Nuclear magnetic resonance in inhomogeneous magnetic fields. *J. Magn. Reson.*, **2000**, *145*, 246-58.
- [78] Blümich, B.; Blumler, P.; Eidmann, G.; Guthausen, A.; Haken, R.; Schmitz, U.; Saito, K.; Zimmer, G. The NMR-mouse: Construction, excitation, and applications. *Magn. Reson. Imaging*, **1998**, *16*, 479-84.
- [79] Guthausen, A.; Zimmer, G.; Blumler, P.; Blümich, B. Analysis of polymer materials by surface NMR via the MOUSE. *J. Magn. Reson.*, **1998**, *130*, 1-7.
- [80] Prado, P.J.; Blümich, B.; Schmitz, U. One-dimensional imaging with a palm-size probe. *J. Magn. Reson.*, **2000**, *144*, 200-06.
- [81] Hahn, E.L. Spin echoes. *Phys. Rev.*, **1950**, *80*, 580-94.
- [82] Carr, H.Y.; Purcell, E.M. Effects of diffusion on free precession in nuclear magnetic resonance experiments. *Phys. Rev.*, **1954**, *94*, 630-38.
- [83] Bloom, A.L. Nuclear induction in inhomogeneous fields. *Phys. Rev.*, **1955**, *98*, 1105-11.
- [84] Antonijevic, S.; Wimperis, S. High-resolution NMR spectroscopy in inhomogeneous B_0 and B_1 fields by two-dimensional correlation. *Chem. Phys. Lett.*, **2003**, *381*, 634-41.
- [85] Freeman, R.; Frenkiel, T.A.; Levitt, M.H. Composite z-pulses. *J. Magn. Reson.*, **1981**, *44*, 409-12.
- [86] Jerschow, A. Multiple echoes initiated by a single radio frequency pulse in NMR. *Chem. Phys. Lett.*, **1998**, *296*, 466-70.

- [87] Ardelean, I.; Scharfenecker, A.; Kimmich, R. Two-pulse nutation echoes generated by gradients of the radiofrequency amplitude and of the main magnetic field. *J. Magn. Reson.*, **2000**, *144*, 45-52.
- [88] Ardelean, I.; Kimmich, R.; Klemm, A. The nutation spin echo and its use for localized NMR. *J. Magn. Reson.*, **2000**, *146*, 43-48.
- [89] Tannus, A.; Garwood, M. Adiabatic pulses. *NMR Biomed.*, **1997**, *10*, 423-34.
- [90] DeGraaf, R.A.; Nicolay, K. Adiabatic rf pulses: Applications to *in vivo* NMR. *Concepts Magn. Reson.*, **1997**, *9*, 247-68.
- [91] Topgaard, D.; Martin, R.W.; Sakellariou, D.; Meriles, C.A.; Pines, A. "Shim pulses" for NMR spectroscopy and imaging. *Proc. Natl. Acad. Sci. USA*, **2004**, *101*, 17576-81.
- [92] Frydman, L.; Lupulescu, A.; Scherf, T. Principles and features of single-scan two-dimensional NMR spectroscopy. *J. Am. Chem. Soc.*, **2003**, *125*, 9204-17.
- [93] Frydman, L.; Scherf, T.; Lupulescu, A. The acquisition of multidimensional NMR spectra within a single scan. *Proc. Natl. Acad. Sci. USA*, **2002**, *99*, 15858-62.
- [94] Shapira, B.; Lupulescu, A.; Shrot, Y.; Frydman, L. Line shape considerations in ultrafast 2D NMR. *J. Magn. Reson.*, **2004**, *166*, 152-63.
- [95] Shrot, Y.; Shapira, B.; Frydman, L. Ultrafast 2D NMR spectroscopy using a continuous spatial encoding of the spin interactions. *J. Magn. Reson.*, **2004**, *171*, 163-70.
- [96] Tal, A.; Shapira, B.; Frydman, L. A continuous phase-modulated approach to spatial encoding in ultrafast 2D NMR spectroscopy. *J. Magn. Reson.*, **2005**, *176*, 107-14.
- [97] Pelupessy, P. Adiabatic single scan two-dimensional NMR spectroscopy. *J. Am. Chem. Soc.*, **2003**, *125*, 12345-50.
- [98] Mollova, E.T.; Metzler, D.E.; Kintanar, A.; Kagamiyama, H.; Hayashi, H.; Hirotsu, K.; Miyahara, I. Use of ^1H - ^{15}N heteronuclear multiple-quantum coherence NMR spectroscopy to study the active site of aspartate aminotransferase. *Biochemistry*, **1997**, *36*, 615-25.
- [99] Sersa, I.; Macura, S. Improvement of spectral resolution by spectroscopic imaging. *Appl. Magn. Reson.*, **2004**, *27*, 259-66.
- [100] de Graaf, R.A.; Rothman, D.L.; Behar, K.L. High resolution NMR spectroscopy of rat brain *in vivo* through indirect zero-quantum-coherence detection. *J. Magn. Reson.*, **2007**, *187*, 320-26.
- [101] Shannon, K.L.; Branca, R.T.; Galiana, G.; Cenzano, S.; Bouchard, L.S.; Soboyejo, W.; Warren, W.S. Simultaneous acquisition of multiple orders of intermolecular multiple-quantum coherence images *in vivo*. *Magn. Reson. Imaging*, **2004**, *22*, 1407-12.
- [102] Rizi, R.R.; Ahn, S.; Alsop, D.C.; Garrett-Roe, S.; Mescher, M.; Richter, W.; Schnall, M.D.; Leigh, J.S.; Warren, W.S. Intermolecular zero-quantum coherence imaging of the human brain. *Magn. Reson. Med.*, **2000**, *43*, 627-32.
- [103] Faber, C.; Pracht, E.; Haase, A. Resolution enhancement in *in vivo* NMR spectroscopy: detection of intermolecular zero-quantum coherences. *J. Magn. Reson.*, **2003**, *161*, 265-74.
- [104] Vroemen, M.; Vroemen, M.; Behr, V.; Neuberger, T.; Jakob, P.; Haase, A.; Schuierer, G.; Bogdahn, U.; Faber, C.; Weidner, N. *In vivo* high-resolution MR imaging of neuropathologic changes in the injured rat spinal cord. *Am. J. Neuroradiol.*, **2006**, *27*, 598-604.
- [105] Balla, D.Z.; Faber, C. *In vivo* intermolecular zero-quantum coherence MR spectroscopy in the rat spinal cord at 17.6 T: A feasibility study. *Magn. Reson. Mater. Phys. Biol. Med.*, **2007**, *20*, 183-91.